Archaeol Anthropol Sci (2018) 10:1359–1373
DOI 10.1007/s12520-016-0457-2

ORIGINAL PAPER

X-ray and neutron-based non-invasive analysis of prehistoric stone artefacts: a contribution to understand mobility and interaction networks

M. I. Dias[1] · Z. S. Kasztovszky[2] · M. I. Prudêncio[1] · A. C. Valera[3] · B. Maróti[2] · I. Harsányi[2] · I. Kovács[4] · Z. Szokefalvi-Nagy[4]

Received: 15 July 2016 / Accepted: 20 December 2016 / Published online: 11 January 2017

Abstract Carbonate-rich archaeological artefacts are difficult to identify and correlate between them and with raw materials of such heterogeneous geological sources, especially when only non-invasive analysis is possible. A novel combination of X-ray and neutron-based non-invasive analysis is implemented and used for the first time to study prehistoric stone idols and vessels, contributing to culture identity, mobility and interaction in the recent Prehistory of Southern Iberia. Elemental composition was obtained by prompt gamma activation analysis (PGAA) and external beam particle-induced x-ray emission (PIXE); homogeneity of the stone artefacts and the presence/absence of internal fractures were obtained by neutron radiography (NR). These atomic and nuclear techniques, simultaneously used for complementary chemical information, have been demonstrated to be of great value as they provide non-destructive compositional information avoiding sample preparation, crucial in so singular and rare objects. The obtained results, especially of PGAA, are very promising and useful in general assessments of provenance. The stone artefacts show signs of both nearby and long-distance procurement, as well as of unknown attribution.

Keywords PGAA · PIXE · Neutron radiography · Stone artefacts · Prehistoric networks · Provenance

✉ M. I. Dias
isadias@ctn.tecnico.ulisboa.pt

[1] Centro de Ciências e Tecnologias Nucleares—C2TN. Campus Tecnológico e Nuclear. Instituto Superior Técnico, Polo de Loures, Estrada Nacional 10 (km 139.7). 2695-066 Bobadela, Loures, Portugal

[2] Centre for Energy Research, Hungarian Academy of Sciences, Budapest, Hungary

[3] Era Arqueologia, Núcleo de Investigação Arqueológica—NIA. Cç. de Santa Catarina, 9C, 1495-705 Cruz Quebrada—Dafundo—Portugal. Interdisciplinary Center for Archaeology and Evolution of Human Behavior (ICArHEB, Universidade do Algarve, Campo de Gambelas, Faro, Portugal

[4] Institute for Particle and Nuclear Physics, Wigner Research Centre for Physics, Hungarian Academy of Sciences, Budapest, Hungary

Introduction

Interaction always assumed a relevant role in the explanation of social organization and social change. During the late fourth and the third millennium BC (at least until its last quarter), Southwest Iberian societies were engaged in a social trajectory of increasing complexity where regional and interregional interaction was a major element. In this context, in southwest Iberia during the late fourth and the third millennium BC, the large ditched enclosures emerge as one type of places that concentrate evidences of large- and middle-scale exchange, becoming important contexts to approach its dynamics in the global social trajectory. Amongst the several known, Perdigões, due to the nature of its contexts, heritage situation and programmed research, provides a good documental base for this enquiry.

The Perdigões site is one of the largest known Portuguese Late Neolithic and Chalcolithic ditched enclosures, occupied during the late fourth to third millennium BC (Valera et al. 2014a, b) in the Reguengos de Monsaraz region, south of Portugal. Several funerary contexts have been excavated dating from the Neolithic and Chalcolithic (fourth and third millennium BC),

providing a variety of exogenous objects comprising pottery, lithic artefacts, stone and bone and ivory idols, pecten shells, etc. (Valera 2012a, b, 2015).

Those materialities, such as artefacts, raw materials, contexts and spatial locations, allow us to speak about the circulation of concrete objects and raw materials, but also of abstractions such as ideas, traditions, technologic knowledge, styles or aesthetics. To deal with these issues, a project was recently designed designated "Mobility and interaction in South Portugal Recent Prehistory: the role of aggregation centres", in the context of which this approach to the assemblage of stone idols and pots was developed.

Scientific data on the composition and provenance of ornamental stones of individual monuments and archaeological objects are becoming increasingly available. For the Iberian Peninsula, many studies have dealt with the distribution and characterization of ornamental stones especially for Roman chronologies but using destructive techniques of analysis (i.e. Cabral et al. 1992; Lapuente 1995; Lapuente and Turi 1995; Morbidelli et al. 2007; Domínguez Bella 2009; Origlia et al. 2011; Beltrán et al. 2012; Mañas Romero 2012; Taelman et al. 2013; Taelman 2014).

For prehistoric stone artefacts, there is a lack of archaeometric studies that could complete the stylistic approaches that have been done to Southwest Iberia (Hurtado 2008, 2010). Only for the Chalcolithic site La Pijotilla a mineralogical and typological characterization of cultural calcareous objects was performed. In this study, portable and non-destructive spectral reflectance VIS-short-wave infrared hyperspectral reflectance (SWIR) (400-2500 nm) measurements were applied to both artefacts and samples of calcareous quarries surrounding the archaeological site (Polvorinos del Río et al. 2010). Also, X-ray diffraction and petrography was done in the geological samples. Interesting results were obtained with the attribution of idols to calcitic marbles, most probably from Alconera quarry, even for some objects, respectively, some eye-decorated and betilo idols, Sierra de Almendral and Nogales were not discarded.

Stone idols from the Perdigões archaeological site have different typologies and apparently are mostly made of marble or limestone, suggesting different origins for these artefacts, since none of the rocks occur locally but regionally. Some questions remain unanswered, such as their compositional nature and their provenance and related outcrops (if possible), contributing to understanding the interaction network in which Perdigões was involved.

This work is, to our best knowledge, the first determination of the chemical composition of both bulk material and surface of prehistoric stone idols and vessels from Iberian Peninsula.

Sourcing carbonate-rich artefacts is problematic, especially because macroscopically they may look similar, even if they come from different sources, and from a mineralogical point of view, they are almost pure $CaCO_3$ with a very heterogeneous mixture of impurities. Similarly, to sourcing microcrystalline quartz (Crandell 2012) and silex artefact (Prudêncio et al. 2016), in the case of carbonate artefacts, especially those deriving from the metamorphic evolution of previous carbonates (marbles), similarity arises between them in many respects (i.e. mineralogical, physical–structural and chemical), and a significant overlap with other sources may occur due to the fact that impurities are generally heterogeneous in this kind of geological source.

The application of trace element and isotope geochemistry of strontium to studies of carbonate diagenesis is a well-established method (Banner 1995) and a powerful tool. Also, several studies comprising minero-petrographic and isotopic studies of marble quarries and objects were done (Koralay and Kilinçarslan 2015; Attanasio et al. 2015, Ulens et al. 1994). Unfortunately, the use of radiogenic isotopes implies destructive techniques of analysis, impossible to apply in so rare prehistoric artefacts. So, it is also relevant to evaluate the success of the combination of X-ray and neutron-based non-invasive techniques, like prompt gamma activation analyses (PGAA), external beam particle-induced X-ray emission (PIXE) and neutron radiography (NR), to trace the source(s) of these Chalcolithic artefacts made of carbonate-rich raw materials. These nuclear analytical techniques have been successfully applied to characterize archaeological objects made of various rocks, especially, because of their non-destructive feature (Kasztovszky et al. 2008; Crandell 2012).

PGAA is one of the new techniques available to deal with this problem. Its basis is the radioactive capture of neutrons or the (n,γ) reaction. During this nuclear reaction, an atomic nucleus captures a thermal or subthermal neutron and emits a number of gamma photons promptly (Révay and Belgya 2004). Because of the low intensity of external neutron beams, PGAA can be considered non-destructive. Furthermore, the method does not require sample preparation, since the intact object is positioned directly in the neutron beam. In most cases, no significant long-lived radioisotopes are produced during the analysis. After some days of cooling, the analysed artefacts are in perfect conditions to be returned to museums, collectors and researchers. Due to the high penetrability of the neutron, PGAA gives the composition of the bulk material, thus when comparing the results from PGAA and PIXE, comparison of inner and surface composition of the objects can be made. Furthermore, NR was used to visualize the hidden inner structure of the objects.

Materials and methods

Archaeological stone artefacts and contexts

Thirteen stone idols from the cremation contexts from Pit 40 and one votive vessel from the tholoi Tomb 1 were analysed by PGAA, PIXE and neutron radiography (NR). Additionally, four more stone vases were studied by PIXE and NR (Fig. 1). The contexts from Pit 40 (Fig. 2) are not yet dated and the contexts from Tomb 1 were dated between 2800 and 2500 BC (Valera et al. 2014b).

The raw materials

Most of the carbonate rocks in Portugal occur near the shore (north of Lisbon and Algarve), particularly limestones, or in Alentejo region, particularly marbles. The main mining district of ornamental limestones is the Mesozoic Maciço Calcário Estremenho (MCE), located 150 km north of Lisbon, and the region of Pêro Pinheiro, close to Lisbon, where there are signs of quarrying since the Roman times. Also, in the Algarve region, there is exploitation of ornamental stones. Regarding marbles, they occur mainly in the Alentejo region, being the Anticlinal de Estremoz the main production centre, where there are also evidence of quarrying since 370 BC (Martins and Lopes 2011).

Taking into consideration archaeological and geological considerations, possible geological sources for the studied stone artefacts were separated into three categories:

1. Nearby sources (~40 km—the so-called marble triangle Estremoz–Borba–Vila Viçosa, in Alentejo's northeast, contains Portugal's most important ornamental rock deposit)
2. Moderate distance areas (~130 km—limestone "breccia" from Tavira, Algarve)
3. Remote areas (160 to 220 km—"lioz" limestones from Pêro Pinheiro, "moleanos" limestone from Maciço Calcário Estremenho).

A total of 11 geological samples were analysed, 7 limestones (Moleanos limestone: MOL-1, MOL-2, MOL-3; Lioz limestone: LIOZ-1, LIOZ-2, LIOZ-3; Tavira breccia BT) and 4 marbles (MNR, MAL, MBC, MER).

For both artefacts and geological materials, the same methodological approach was used, so using the same variables, a better comparison and provenance ascription are achieved.

The X-ray method

PIXE spectroscopy is a non-destructive elemental analytical technique. The sample to be studied is bombarded by an energetic particle beam (2–4 MeV proton beams in most cases)

Fig. 1 Stone idols and stone vessels from Perdigões Prehistoric archaeological site. Correspondences to Table 1: 1-PDI 12; 5-PDI 6; 6-PDI 1; 7-PDI 7; 8-PDI 11; 9-PDI 13. Archaeological context: *3* Not analysed limestone items from Tomb 2; *4* not analysed limestone items from Tomb 1. All the rest from Pit 40

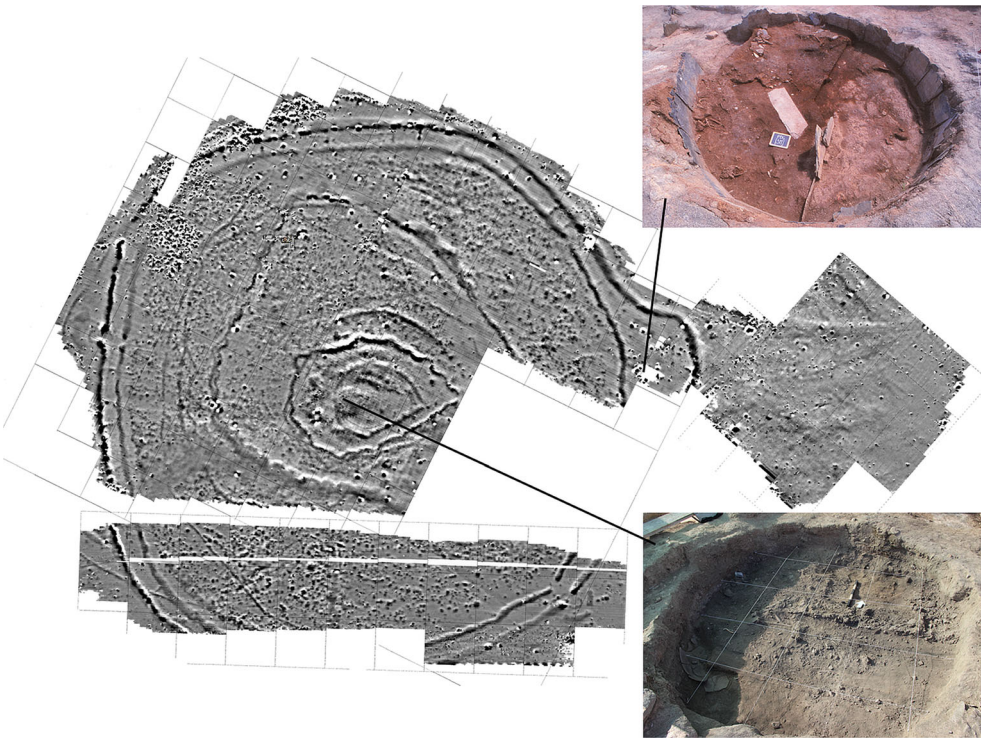

Fig. 2 Location of Tomb 1 and Pit 40 respectively at the eastern extremity and in the centre of Perdigões enclosure

produced by a particle accelerator. The energetic protons ionize also the inner electron shells of the atoms in the bombarded volume and in the electron re-arrangement process, characteristic X-rays are also emitted. The energies of these X-rays are strictly determined by the atomic number of the emitting element, while the intensities of the X-rays are related to its concentration. Because of the intensive slowing down of the bombarding protons in matter and the absorption of the outgoing X-rays, PIXE is inherently sensitive for the surface layers of thicknesses up to some tens of micrometres. In principle, elements from Al to U can simultaneously be detected using a conventional energy-dispersive X-ray detector, and elemental sensitivities down to ppm levels can be achieved in favourable conditions. In the so-called external-beam version of PIXE, the protons are extracted to air through a properly thin exit foil, allowing non-destructive qualitative and quantitative elemental analysis of samples of practically any sizes. This method is especially useful for the non-destructive study of unique and valuable cultural heritage objects, (e.g. archaeological findings and artworks objects) (Gyódi et al. 1999; Rehren et al. 2013).

The PIXE method is very similar to the more well-known standard X-ray fluorescence (XRF) spectroscopy; technically, they differ in the mode of inner shell ionization, only. In XRF, electromagnetic radiation (X-rays from X-ray tube or proper radioactive sources) does it by photo effect, while in PIXE, the energetic charged ions ionize by Coulomb interaction. Due to this important difference, however, PIXE is more sensitive for the lighter elements while in XRF, the closer the absorption edge of a particular element to the energy of the X-ray peaks of the tube, the higher the ionization cross sections. The background caused by scattering of the continuous bremsstrahlung radiation and the scattered exciting peaks also deteriorate the sensitivity of XRF for lighter elements. In addition, the analysed spot could be much smaller, allowing better lateral resolution by PIXE compared especially to that of portable XRF spectrometers. The obvious disadvantages of PIXE, namely the need of access to an accelerator and the necessary transport of the valuable cultural heritage object are not relevant in our case since the Budapest Research Reactor for the neutron studies and the external beam PIXE facility locate in the same campus, and they were available simultaneously as the common infrastructure of the CHARISMA Wigner BNC platform.

The PIXE measurements were performed at the 5MV Van de Graaff accelerator of the Institute of Particle and Nuclear Physics, Wigner Research Centre for Physics of Hungarian Academy of Sciences. Proton beam of 2.5 MeV energy was extracted from the evacuated beam pipe to air through a 7.5-m thick Kapton foil. Target-window distance of 10 mm was chosen at which distance the beam diameter was found to be about 1 mm. The objects to be analysed were put on a computer-controlled stage enabling accurate three-dimensional positioning. A mechanical pointing device helped the proper adjustment of the selected target spot. External beam currents in the range of 1–5 nA were used. Characteristic X-ray spectra were taken by an AMPTEK X-123 X-ray spectrometer. The energy resolution of the

25 mm2 × 500 μm SDD detector was 125 eV for the Mn Kα line. The detector was positioned at 135° with respect to the beam direction. To reduce low-energy X-ray counts, an Al absorber of 100-μm thickness was applied in front of the detector. The net X-ray peak intensities and the concentration calculations were made by the offline GUPIX program package (Campbell et al. 2000).

Neutron-based methods

The experiments have been performed at the PGAA (Szentmiklósi et al. 2010) and NIPS–NORMA (Kis et al. 2015) instruments installed on a guided cold-neutron beam of the Budapest Research Reactor. In a PGAA experiment, the sample is irradiated with cold neutrons, and the prompt and delayed gamma photons emitted by the target nuclei are measured simultaneously The method is applicable mostly to quantify almost all the major and minor components (H, Na, K, Mg, Al, Si, Ti, Mn, Fe and Cl) and some trace elements (B is an important one, occasionally also Cr, Sc, V, Nd, Sm and Gd) in silica-based samples of geological origin, such as limestone. Since oxygen is a poorly detectable element, the concentrations of the major components' oxides are calculated based on their oxidation numbers.

The typical thermal equivalent neutron flux in the sample position of the PGAA and NIPS–NORMA station is 7.6×10^7 and 2.2×10^7 cm^{-2} s^{-1}, respectively. The prompt and delayed gamma photons are detected using a Compton-suppressed HPGe detector. The analysed sample volume depends on the solid angle of the applied detector and on the size of the neutron beam. The neutrons are highly penetrating particles, and the elements of interest have high energy gammas (e.g. above 2 MeV); therefore, the PGAA measurements provide the average bulk composition of few centimetre-thick objects. During the analysis of the limestone samples, the typical acquisition time varied between 2300 and 8300 s, in order to collect statistically significant counts. Between the sample chamber and the HPGe detector, lead gamma-ray collimator was applied with a diameter of 30 mm, while the neutron beam was reduced to 24 or 44 mm^2 using a ^{6}Li-enriched polymer neutron collimator, to keep the count rate at appropriate level. The collected spectra have been evaluated with the Hypermet PC software (Fazekas et al. 1997; Révay et al. 2005); the element identification and calculation of concentrations are based on BNC PGAA library (Révay et al. 2004; Révay 2009).

NR can be useful to visualize the inner content of an artefact. Similar to X-ray radiography, neutron radiography is a very efficient tool to enhance investigations in the field of non-destructive testing.

The advantage of neutrons compared to X-rays is the ability to visualize light elements (i.e. with low atomic numbers) such as hydrogen, water, carbon, etc. This property of being easily absorbed by light elements such as hydrogen makes it possible to image, e.g. the distribution of water within a specimen. Neutrons also penetrate heavy elements (i.e. with high atomic numbers) such as lead to study *f* materials in complex sample environments.

The neutron radiographic images were taken at the combined NIPS–NORMA station. The sample chamber is $200 \times 200 \times 200$ mm^3; the samples were placed on a motorized sample stage. The spatial resolution is 0.2–0.5 mm, and the maximum field of view is 48 mm × 48 mm. The detailed description of the NR setup can be found in the literature (Kis et al. 2015).

The radiographic images taken at NORMA require corrections for the beam profile and the detector noise (Anderson et al. 2009; Schindelin et al. 2012; Wavemetric Inc. 2013).

Results and discussion

PIXE was used for quantification of chemical elements of the few 10-μm thick layer of the objects. The analyses were divided according the nature of the object: stone idols—PDI or stone vases—PDV, and according with specific position on each object's surface: stone surface; reddish crust; white cover; bone and soil; bone; brown spot; brownish cover; stone interior. Selected PIXE analysis point on the white cover of a stone idol and that on the stone surface of a vase are shown in Fig. 3a, b , respectively. The points were properly positioned by the pull-out aiming pin. The horizontal cone-shaped tube with the yellow Kapton exit foil and the aslope X-ray detector with the Al absorber foil are also clearly seen in both pictures.

PIXE results are listed in Table 1. The geochemical assay of the stone idols' surface shows calcium oxide contents ranging from 39.41 to 71.30%, which is because a limestone is primarily calcite. The calcium oxide contents show a negative correlation with silica which is based on the fact that calcium oxides from calcite and silica oxide from quartz are forming two different mineral phases that are not related. This SiO_2–CaO negative correlation is usually attributed to chemical diagenetic replacement during the limestone deposition environment (Ehinola et al. 2016). Silica oxide on the stone idols' surface ranges from non-detected to 21.52%, with an average of 13%. The silica contents are explained by the existing impurities in both the limestone and the surface of the artefacts (soil remains). Manganese oxide on the stone surface has values ranging from non-detectable to 0.015%, and iron oxide values are also generally low

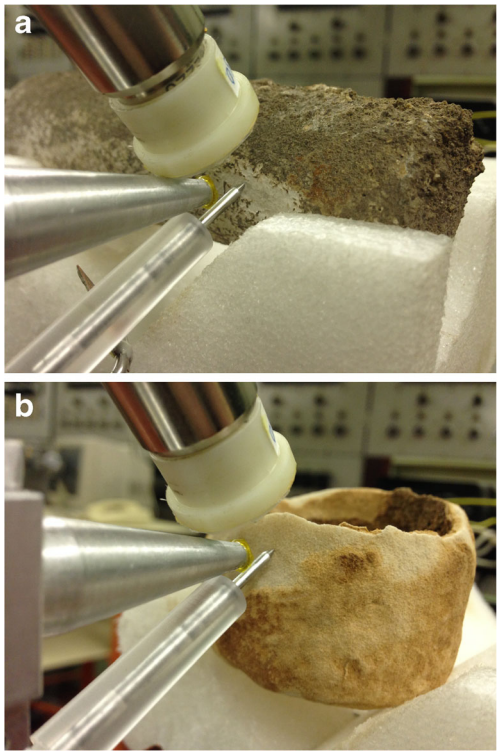

Fig. 3 Selected PIXE analysis point on the white cover of a stone idol and that on the stone surface of a vase are shown in **a** and **b**, respectively

from 0.07 to 3.99%, which means a general low oxidizing effect in the depositional environment of the raw material. In general, the vases have lower contents of calcium (Fig. 4), with the exception of vase PDV7. The dotted ellipse of Fig. 4 comprises mostly vases, with lower amounts of calcium and with no negative correlation between calcium and silica oxides, which may be due to their different surface when compared with idols, enriched in soil residues and crusts and also to different raw material. The strong increase of iron, silica, manganese and phosphorous in the reddish/brownish crusts and bones and soil residues (Fig. 5) suggests that the high iron values found in this points may be due to surface enrichment of soil contamination, and the high phosphorous values to bone contribution. The white covers have more calcium contents than those of the surrounding measured points (Fig. 4), suggesting that a special procedure was taken preparing a white cover probably made of pure calcium carbonate. It is also interesting to emphasize that the interior of some vases has a brownish crust, and also bone remains with much higher phosphorous content, together with iron, manganese, zinc and copper.

Neutron radiography was used to reveal morphological and/or structural information related with stone artefacts. The raw material of the objects turned out to be homogeneous, but it was possible to observe fissures and fractures in them. On the other hand, images obtained from the stone vessels were very interesting, giving a complete idea of the "making of the pot", particularly the thickness of both bottom and lateral walls (Fig. 6b). Additionally, highly neutron-absorbing material was identified on the inner surface of the stone vessel. It is assumed to be either hydrogen containing organic material. However, this contrast can be caused by the high Fe-containing terrigenous cover on the inner surface detected by the PIXE method.

PGAA applied on both stone artefacts from Perdigões and potential raw materials provided chemical data used to differentiate and/or correlate in a compositional point of view, both artefacts and geological sources. Idols have not been cleaned from surface deposits, particularly enriched in crashed bones and soil. Results discussion took into consideration if analysed chemical contents might have been enlarged due to bone contamination and not specifically to the nature of geological source, but no correlation was directly established between the analysed artefacts, and the chemical contents that are usually present in bones and also used for paleonutrition research (Allmäe et al. 2012).

The oxide/element concentrations measured by PGAA were used accordingly; they were above the quantification limit in most of the samples, i.e. CaO, CO_2, LOI (H_2O), SiO_2, Fe_2O_3t, MnO, K_2O, MgO, B, TiO_2, Cl, Sm and Gd (Table 2).

To categorize the stone artefacts and geological samples, a classical chemical parameter of limestones (Todd 1966) and marbles (Rosen et al. 2007; Goldschmidth et al. 1955; Onimisi et al. 2013) has been applied, with the use of the Ca and Mg proportion, the distribution of Ca/Mg and its reciprocal Mg/Ca ratio. In the studied samples, CaO is the prevailing major component, ranging from 50 and 57 wt% in artefact samples, and between ~51 and ~56 wt% in the geological samples. All analysed samples have a relatively low MgO concentration (<2%). Mg/Ca ratios in geological samples vary from 0.029 to 0.009% and in artefacts from 0.01% to 0.007%. The potential raw materials are all calcitic-type marbles and pure limestones, but the breccia Tavira sample (BT) is a limestone more enriched in Mg, and the Ruivina marble is more silica enriched. Regarding the artefact samples, they are all pure limestones or calcitic-type marbles. The Lioz limestones have in general lower Mg/Ca ratios. It is also interesting to notice in the marbles evidences of a possible flow of titanium due to the breakdown of biotite into the recrystallizing carbonates during metamorphism. The smaller but appreciable concentration of manganese in carbonates is probably attributable to similarity in ionic size with ion Ca^{2+}, where a substitution of Mn by Ca might have occurred. The other oxide contents are generally low. The concentration of the total alkalis ($Na_2O + K_2O$) in the carbonate bodies is very low, less than 1%, which is similar to the alkali content of typical marble bodies. Also, the other oxides (Al_2O_3 and Fe_2O_3) are generally low, less than 1%,

Table 1 Composition of the stone artefacts in weight percentage of oxides according to the PIXE results

Sample	analysis location		Si	P	K	Ca	Ti	Mn	Fe	Ni	Cu	Zn
PDI-1	Stone surface	wt%	ND	15.11	0.07	46.12	0.10	0.11	0.30	ND	ND	0.03
		Rel. Unc.%		2.96	19.35	0.35	8.46	6.89	4.09			17.91
PDI-1	Reddish “crust”	wt%	ND	16.31	0.13	43.86	0.10	0.09	0.56	ND	ND	0.05
		Rel. Unc.%		2.99	12.79	0.38	9.53	8.51	3.22			16.62
PDI-1	White cover	wt%	ND	ND	0.03	71.14	0.05	0.03	0.20	ND	ND	ND
		Rel. Unc.%			42.39	0.31	23.65	22.99	6.26			62.81
PDI-1	Bone&soil residues	wt%	ND	6.96	2.38	51.24	1.19	0.46	5.25	ND	ND	0.05
		Rel. Unc.%		5.90	1.49	0.35	2.35	22.99	6.26			17.68
PDI-1	White cover	wt%	ND	19.02	ND	40.24	ND	ND	0.05	ND	ND	0.02
		Rel. Unc.%		2.78		0.32			7.50			17.68
PDI-1	Stone surface	wt%	ND	ND	0.61	67.28	0.46	0.15	3.20	ND	ND	ND
		Rel. Unc.%			3.35	0.31	4.70	8.36	1.56			
PDI-1	Reddish spot	wt%	4.27	16.32	0.25	37.36	0.08	0.08	0.49	ND	ND	0.03
		Rel. Unc.%	14.71	2.39	5.33	0.27	7.33	6.29	2.51			15.59
PDI-1	White cover	wt%	3.01	ND	0.09	66.67	0.03	0.01	0.08	ND	ND	ND
		Rel. Unc.%	26.50		9.74	0.19	17.34	23.08	7.06			
PDI-1	Grey spot (contaminated by roots inprints)	wt%	7.34	ND	0.35	58.80	0.14	0.41	0.67	ND	ND	ND
		Rel. Unc.%	13.26		4.03	0.23	7.14	3.38	2.86			
PDI-2	White cover	wt%	2.73	ND	0.04	67.08	0.03	0.03	0.13	ND	ND	ND
		Rel. Unc.%	29.53		19.92	0.20	19.55	11.99	4.74			
PDI-2	Stone surface	wt%	11.70	ND	0.53	51.35	0.23	0.08	1.56	ND	0.01	0.01
		Rel. Unc.%	9.68		1.77	0.17	2.30	3.88	0.81		23.93	18.17
PDI-3	Stone fracture (inner part)	wt%	ND	ND	ND	71.04	0.06	ND	0.28	0.04	ND	ND
		Rel. Unc.%				0.29	18.34	1.56	4.96	33.70		
PDI-3	Stone surface	wt%	ND	ND	0.87	65.55	0.96	0.22	3.99	0.05	0.02	ND
		Rel. Unc.%			2.34	0.30	2.62	5.75	1.21	27.75	25.83	
PDI-3	Bone& soil residues	wt%	ND	ND	2.08	53.70	1.77	0.32	11.80	ND	ND	ND
		Rel. Unc.%			2.28	0.48	2.81	7.73	1.08			
PDI-4	Stone surface	wt%	6.19	1.31	0.17	59.11	0.10	0.05	0.47	ND	ND	ND
		Rel. Unc.%	12.65	23.99	5.72	0.19	6.39	8.57	2.41			
PDI-5	White cover	wt%	ND	ND	ND	69.25	ND	0.01	0.11	ND	ND	ND
		Rel. Unc.%				0.24		32.36	8.76			
PDI-6	Stone surface (whitish)	wt%	ND	ND	ND	71.30	ND	0.02	0.09	0.03	ND	ND
		Rel. Unc.%				0.27		21.98	6.45	31.99		
PDI-6	Brown spot	wt%	1.51	19.42	0.10	37.03	0.04	0.01	0.17	ND	ND	0.03
		Rel. Unc.%	25.72	1.65	6.85	0.20	7.21	13.78	2.41			11.03
PDI-6	Stone surface (whitish)	wt%	ND	ND	0.05	68.10	ND	0.01	0.07	ND	0.00	ND
		Rel. Unc.%			17.75	0.18		21.21	7.32			
PDI-7	Bone close to soil residues	wt%	ND	15.44	ND	46.15	ND	0.02	0.03	ND	ND	ND
		Rel. Unc.%		3.22		0.36		22.53	23.52			
PDI-7	Soil residues close to bone	wt%	ND	ND	ND	69.69	ND	ND	1.86	ND	ND	ND
		Rel. Unc.%				0.38			4.35			
PDI-7	White cover	wt%	ND	ND	ND	71.49	ND	ND	0.24	ND	ND	ND
		Rel. Unc.%				0.34			10.49			
PDI-7	Brown-redish spot	wt%	ND	10.58	ND	53.44	ND	0.10	0.68	ND	ND	ND
		Rel. Unc.%		1.84		0.32		9.90	3.52			
PDI-8	Grey spot	wt%	19.77	ND	0.59	38.69	0.26	0.08	1.81	ND	ND	0.01

Table 1 (continued)

Sample	analysis location		Si	P	K	Ca	Ti	Mn	Fe	Ni	Cu	Zn
		Rel. Unc.%	3.91		1.78	0.21	2.24	4.20	0.84			17.96
PDI-8	Whitish spots	wt%	12.31	ND	0.32	50.43	0.12	0.06	0.79	ND	ND	0.02
		Rel. Unc.%	6.49	49.57	3.43	0.20	4.99	6.84	1.71			19.96
PDI-8	Whitish spots	wt%	11.73	ND	0.14	53.04	0.05	0.03	0.32	ND	ND	0.01
		Rel. Unc.%	6.13		5.76	0.18	8.39	9.14	2.24			28.41
PDI-9	Whitish spots	wt%	8.85	ND	0.17	57.22	0.07	0.08	0.44	ND	ND	ND
		Rel. Unc.%	9.68		6.14	0.22	8.64	6.56	2.73			
PDI-9	Grey spot	wt%	11.26	9.52	0.38	37.19	0.14	0.23	0.81	ND	ND	0.02
		Rel. Unc.%	5.78	2.93	2.86	0.24	3.80	2.68	1.53			14.81
PDI-9	Whitish spots	wt%	7.01	ND	0.29	60.15	0.07	0.03	0.26	ND	ND	ND
		Rel. Unc.%	12.16		3.88	0.20	9.39	11.72	3.65			
PDI-10	Whitish spots	wt%	11.30	ND	0.27	53.30	0.09	0.03	0.56	ND	ND	0.02
		Rel. Unc.%	8.12		4.53	0.23	7.64	14.99	2.58			
PDI-10	Stone cover	wt%	12.12	ND	0.35	51.90	0.10	0.03	0.65	ND	ND	0.01
		Rel. Unc.%	7.36		3.67	0.23	7.17	12.99	2.31			32.87
PDI-10	Whitish spot	wt%	10.58	ND	0.18	54.97	0.02	ND	0.15	ND	ND	ND
		Rel. Unc.%	9.09		7.04	0.24	27.57		5.90			
PDI-10	Stone surface	wt%	12.94	ND	0.30	51.07	0.05	0.02	0.31	ND	ND	ND
		Rel. Unc.%	7.62		4.73	0.25	13.01	23.47	3.98			
PDI-10	Stone surface	wt%	ND	ND	0.20	65.77	ND	ND	0.20	ND	ND	ND
		Rel. Unc.%			8.11	0.25	38.24	30.84	7.05			
PDI-12	Stone surface	wt%	ND	ND	0.09	70.98	0.05	ND	0.29	0.04	ND	ND
		Rel. Unc.%			15.45	0.33	20.84		4.98	38.14		
PDI-12	Bone close to soil residues	wt%	ND	14.40	ND	47.70	0.01	0.02	0.11	ND	ND	0.02
		Rel. Unc.%		2.28	39.89	0.24	26.13	11.58	3.09			9.86
PDI-12	Soil residues	wt%	ND	ND	0.20	70.22	0.13	0.06	0.83	0.05	ND	0.03
		Rel. Unc.%			6.12	0.28	7.94	9.83	2.13	23.65		17.90
PDI-12	Stone surface	wt%	ND	ND	0.57	69.46	0.19	0.12	1.16	0.05	0.02	0.02
		Rel. Unc.%			2.45	0.28	5.77	5.90	1.68	23.24	25.72	19.49
PDI-13	Stone surface	wt%	20.07	ND	0.49	39.41	0.13	0.09	0.78	ND	ND	ND
		Rel. Unc.%	4.06		2.09	0.22	3.86	4.44	1.50			
PDI-13	Stone surface (more dirty)	wt%	21.52	0.97	1.14	33.39	0.34	0.17	2.24	ND	ND	0.01
		Rel. Unc.%	3.85	24.53	1.36	0.25	2.13	3.16	0.87			28.22
PDI-14	Stone surface	wt%	6.37	ND	0.37	61.13	0.05	0.02	0.23	ND	ND	0.01
		Rel. Unc.%	12.84		3.05	0.21	11.40	14.17	3.59			31.58
PDV-2	Whitish surface	wt%	ND	ND	ND	71.12	ND	0.07	0.33	ND	ND	ND
		Rel. Unc.%				0.18		7.46	3.12			
PDV-2	Brownish terrigenous cover (exterior)	wt%	ND	15.32	ND	43.96	ND	0.30	2.33	ND	ND	ND
		Rel. Unc.%		2.26		0.20		2.45	0.91			
PDV-3	Brownish terrigenous cover (interior)	wt%	ND	13.21	ND	28.75	ND	1.75	20.98	ND	0.05	0.17
		Rel. Unc.%	5.28	0.52		2.57		2.57	0.77		33.03	16.81
PDV-3	Stone surface (whitish)	wt%	ND	ND	ND	70.76	ND	0.08	0.69	ND	0.00	ND
		Rel. Unc.%				0.23		9.85	3.18			
PDV-3	Stone surface (brownish)	wt%	ND	10.11	ND	49.94	ND	0.17	5.23	ND	ND	ND
		Rel. Unc.%		4.26		0.28		6.31	1.08			
PDV-4	Stone surface (whitish)	wt%	3.67	ND	0.07	65.41	0.05	0.03	0.32	ND	ND	ND
		Rel. Unc.%	29.67		18.25	0.24	17.40	16.61	4.71			

Table 1 (continued)

Sample	analysis location		Si	P	K	Ca	Ti	Mn	Fe	Ni	Cu	Zn
PDV-4	Stone surface (brownish)	wt%	9.83	14.75	0.56	30.01	0.14	0.67	1.08	ND	ND	0.04
		Rel. Unc.%	6.86	2.57	2.68	0.28	4.69	1.91	1.70			14.76
PDV-4	Brown spot	wt%	7.11	16.50	0.41	30.55	0.10	0.49	1.02	ND	0.01	0.07
		Rel. Unc.%	9.18	2.41	3.62	0.31	5.94	2.35	1.84		24.87	11.52
PDV-5	Stone surface (weathered)	wt%	21.98	3.88	1.31	27.03	0.33	0.04	3.18	ND	0.01	0.02
		Rel. Unc.%	4.13	6.33	1.31	0.25	2.10	7.78	0.72		24.66	19.02
PDV-5	Brownish terrigenous cover (exterior)	wt%	11.94	14.42	0.83	26.68	0.20	0.15	1.92	ND	0.01	0.08
		Rel. Unc.%	6.16	6.16	2.18	0.33	3.77	4.46	1.25		35.03	9.97
PDV-7	Stone surface (whitish)	wt%	6.08	ND	0.07	61.73	0.04	0.04	0.32	ND	ND	ND
		Rel. Unc.%	12.92		12.44	0.19	13.78	9.49	2.92			
PDV-7	Stone surface (brownish)	wt%	17.64	7.79	1.28	27.48	0.30	0.06	2.95	ND	ND	0.05
		Rel. Unc.%	3.90	3.33	1.27	0.22	1.93	5.07	0.64			8.17
PDV-7	Brownish terrigenous cover (interior)	wt%	15.26	11.68	1.18	24.97	0.33	0.16	2.67	ND	ND	0.03
		Rel. Unc.%	4.11	3.41	1.22	0.24	1.76	2.64	0.66		28.86	31.36
Average rel. Unc.%			10.74	7.19	7.81	0.30	9.76	10.51	3.69	29.74	27.74	20.41

ND non-detectable

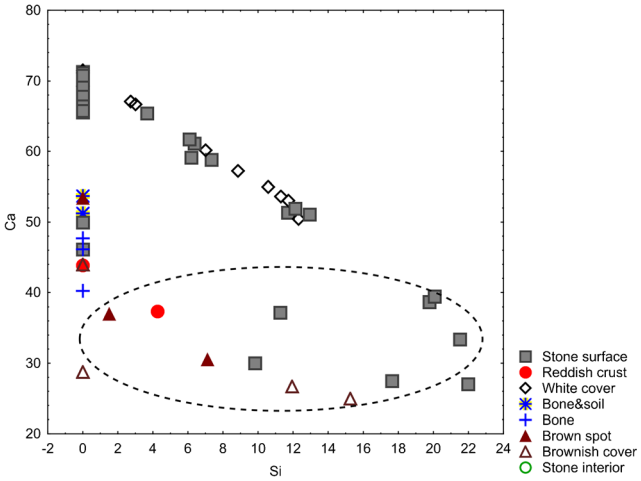

Fig. 4 Relation between calcium and silica concentrations in weight percentage of oxides according with the analysed points of idols and vessel artefacts. *Dotted ellipse* comprises mostly vases

and may be indicative of the absence of aluminosilicates. We can infer loss on ignition (LOI) by the content of volatiles (CO_2, H_2O) present in the samples. The average values of LOI in the studied samples are relatively high, varying from are 42.01 and 46.26% and a positive correlation occurs between CaO and LOI, due to the fact that LOI is generated mainly by the carbonate content of calcite.

Boron contents in limestones are generally low and are due to clay or organic presence, largely incorporated in illite, being used as a paleosalinity indicator and marine environment. Studied marbles have lower contents of B than limestones, and in artefacts, B content has also a varied range, from 0.238 to 2.540 μg/g.

Sedimentary rocks have unique assemblages of trace elements, thus their determination in metamorphic rocks provides a unique way to guess the nature of the premetamorphic material. Immobile trace elements such as the rare-earth elements and the high-field strength

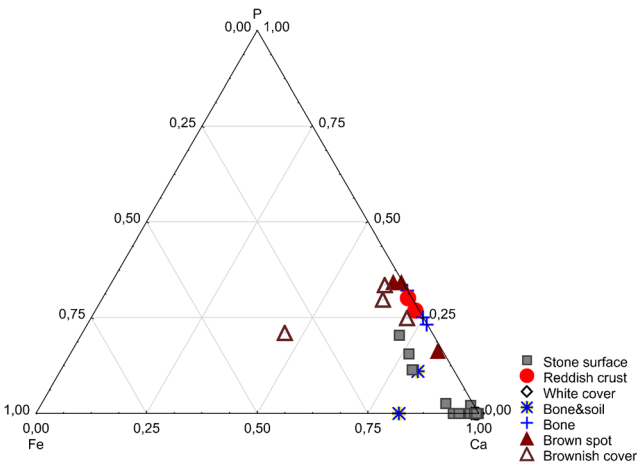

Fig. 5 Triangular composition diagram of iron, phosphorous and calcium concentrations of the analysed points of idols and vessel artefacts

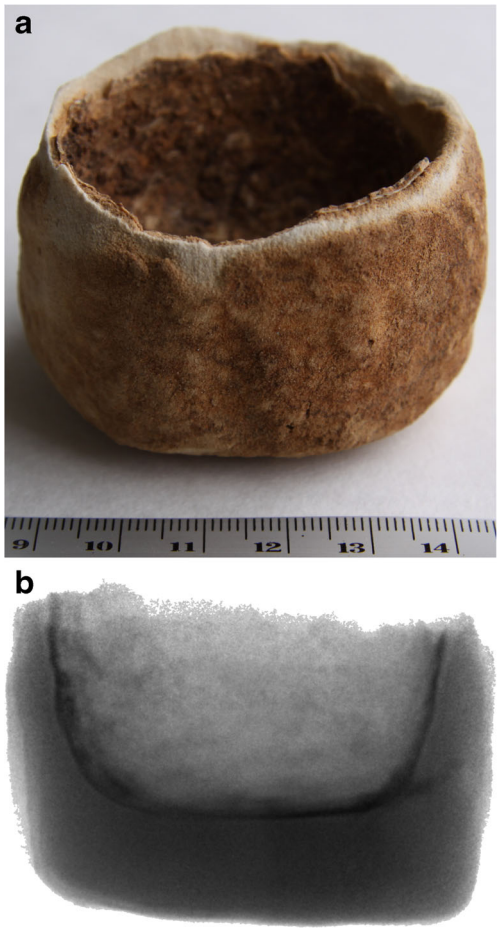

Fig. 6 Stone vessel PDV 3 (**a**) and corresponding neutron radiography image (**b**)

elements are important for provenance determination of pelitic rocks (Taylor and McLennan 1981) because their concentrations often reflect those of their source rock. With PGAA, we have determined Sm and Gd. Gadolinium was detected only in two geological samples, and in a few stone artefacts. No Sm was detected in two idols and in the vase.

A statistical approach was performed with the stone artefacts analysed by PGAA, taking into consideration chemical element as variables. To better estimate compositional groups, cluster analysis (k-means and joining tree clustering methods) and principal component analysis have been done. The division in five "groups" was only used to structure the data (Fig. 7) and better estimate similarities and dissimilarities. Considering the number of samples analysed, most of the "groups" only have two samples, and some of them have only as similarity to be different from the others. Group 1 and 2 differs from the other samples, but also within them, particularly samples PDI 3 and PDI 11. These two artefacts of the so-called group 1 (G1) (PDI 3 and PDI 11) have only in common the low contents of calcium, and they are the only ones where sodium was detected. All the other chemical content differences question the possibility of the same source, like PDI 3 has higher amounts of Ti and Fe, and PDI 11 more Cl content. The G2 "group" (PDI 6 and PDI 14) are the only ones where aluminium was detected. Artefacts from G3 (PDI 2, PDI 5 and PDI 8) have the higher samarium and gadolinium contents. Artefacts from G4 (PDI 10 and PDI 12) have the higher potassium and magnesium contents. G5 artefacts (PDI 1, PDI 4 and PDI 9) differ from the others due to higher amount of calcium and lower of CO2. The two extreme outliers (PDI 13 and PDV 7) removed from the clustering method are differentiated due to the following: in the case of idol PDI 13, it has the higher iron and manganese contents, and the lower samarium content; the vase PDV 7 has high content of H_2O_2, and low contents of titanium and samarium and has the high boron content, pointing to a limestone raw material with higher porosity. As expected, stone artefacts made with higher porosity raw material and high organic matter residues have higher amounts of H_2O and B.

In order to characterize strategies of artefacts manufacture and lithic raw material exploitation, a comparison study was established between the areas of possible sourcing and the stone artefacts, taking into consideration PGAA results (Fig. 8). It is clear the existence of samples with unknown source, corresponding to the abovementioned groups 1 and 2. Samples from the "marble triangle" have chemical heterogeneities that make fingerprinting within them very challenging, especially when dealing with non-destructive methods of analysis, as well as when establishing correlations with artefacts. Nevertheless, it was possible to establish geochemical correlations between geological sources and artefacts: (1) the nearby sources from the "marble triangle" Estremoz–Borba–Vila Viçosa seems to be the most likely the source for artefacts of G3, G4 and G5 (disregarding the Ruivina marble, which is the only one detachable from the others due especially to higher Si and lower Ca contents). (2) The medium distance of the area samples—Tavira Breccia—does not present any chemical affinity with the analysed artefacts. (3) Geological samples from remote areas (MCE limestones–Moleanos and Pêro Pinheiro–Lioz) do not point to be a source for the stone idols; on the other hand, stone vessel (PDV 7) is the only artefact that has chemical similarity with a limestone sample, particularly the Moleanos 2 sample from MCE.

Taking this further, we might theorize that the analysed stone artefacts from Perdigões show signs of both nearby and long-distance procurement, as well as of unknown attribution, like it was already found for the ceramic materials of similar contexts of the

Table 2 Composition of the stone artefacts in weight percentage of oxides according to the PGAA results

Sample	Sample type		H2O	CaO	CO2	Na2O	K2O	MgO	Al2O3	SiO2	P2O5	SO3	TiO2	MnO	Fe2O3	B	Cl	Sm	Gd
PDI-1	*Idol*	wt%	0.220	57	43									0.01	0.05	2.66E−05	0.002	3.85E−06	
		Rel. Unc.%	2.71	2.2	3.0									5.54	6.12	4.88	6.95	10	
PDI-2	*Idol*	wt%	0.627	53	44						1.39			0.02	0.06	7.82E−05	0.002	4.46E−05	
		Rel. Unc.%	2.31	2.2	2.6						7.51			3.80	6.41	2.72	5.87	3.47	
PDI-3	*Idol*	wt%	0.671	51	44	0.06	0.14	0.59		2.94	0.02		0.04	0.02	0.39	0.0003	0.004	3.30E−05	3.22E−05
		Rel. Unc.%	2.47	2.4	2.8	7.07	3.36	6.62		3.21	16.81		3.41	3.13	3.72	2.48	3.34	3.47	11
PDI-4	*Idol*	wt%	0.326	57	41					0.09	1.01			0.01		4.54E−05	0.001	7.16E−06	1.42E−05
		Rel. Unc.%	2.71	2.3	3.3					13.22	6.71			5.51		3.75	9.02	9.41	9.32
PDI-5	*Idol*	wt%	0.251	55	44		0.01	0.21		0.36		0.04	0.02	0.01		6.25E−05	0.005	3.33E−05	3.81E−05
		Rel. Unc.%	2.86	2.4	3.1		9.22	8.21		4.97		9.11	4.25	3.59		3.05	3.95	3.61	8.85
PDI-6	*Idol*	wt%	0.707	53	42		0.06	0.67	0.22	1.72	1.85		0.01	0.02	0.13	0.000	0.003	1.19E−05	
		Rel. Unc.%	2.15	2.0	2.7		3.17	6.04	6.00	3.20	5.72		5.80	3.65	5.03	2256	4336	6.34	
PDI-6	*Idol*	wt%	0.173	56	44				0.60					0.01	0.05	1.94E−05	0.007		
		Rel. Unc.%	2.82	2.3	3.0				3.79					5.60	8.60	3276	3641		
PDI-8	*Idol*	wt%	0.112	54	45									0.01	0.07	2.71E−05		2.95E−05	4.45E−05
		Rel. Unc.%	2.74	2.2	2.6									3.96	6.17	4901		3.98	18.69
PDI-9	*Idol*	wt%	0.254	55	42			0.42		0.85	0.70			0.02	0.07	0.0001			
		Rel. Unc.%	2.48	2.1	2.7			9.04		4.13	9.00			6.00	6.00	2856			
PDI-10	*Idol*	wt%	0.095	54	45		0.03	0.32		0.66			0.004	0.003	0.06	3.39E−05	0.001	7.67E−06	
		Rel. Unc.%	2.98	2.2	2.6		3.93	8.81		3.94			9.10	7.88	5.17	3.86	7397	5.71	
PDI-11	*Idol*	wt%	0.403	50	46	0.05	0.05	0.51		1.24	0.95	0.05	0.02	0.02	0.17	0.0002	0.015	1.75E−05	1.89E−05
		Rel. Unc.%	2.17	2.1	2.4	10.16	3.19	7.32		3.43	6.89	9.09	4.21	3.74	4.24	2.23	2560	4.90	7.07
PDI-12	*Idol*	wt%	0.074	53	45		0.03	0.80		0.58			0.01	0.01	0.06	2.38E−05	0.003	6.56E−06	6.08E−06
		Rel. Unc.%	3.02	2.2	2.6		3.32	6.24		4.28			7.70	6.14	9.65	5.27	5715	8.81	8.09
PDI-13	*Idol*	wt%	0.106	53	46			0.32		0.29			0.01	0.06	0.13	2.52E−05			
		Rel. Unc.%	3.05	2.3	2.7			12.98		8.07			6.90	5.44	3.55	5.78			
PDI-13	*Idol*	wt%	0.170	55	43					0.38				0.08	0.13	4.90E−05		1.20E−05	
		Rel. Unc.%	4.18	2.9	3.8					11.02				3.67	7.73	6.65		11.91	
PDI-14	*Idol*	wt%	0.232	53	43		0.09	0.61	0.31	2.17			0.01	0.01	0.14	0.0001	0.008	1.58E−05	
		Rel. Unc.%	2.20	2.0	2.5		2.81	6.63	4.17	3.04			3.98	4.47	4.31	2.23	2800	4.16	
PDV-7	*Vase*	wt%	0.516	53	45					0.48			0.002	0.02	0.09	0.0001	0.001		
		Rel. Unc.%	2.33	2.2	2.6					4.71			11.42	5.53	5.25	2544	10.719		
MOL-1	*Limestone moleanos*	wt%	0.301	54	45			0.43				0.09				0.0001	0.002	3.28E−05	
		Rel. Unc.%	2.33	2.2	2.6			7.97				6.69				2.59	5598	3.53	
MOL-2	*Limestone moleanos*	wt%	0.844	54	45			0.28				0.05	0.003	0.003		6.48E−05	0.002		
		Rel. Unc.%	2.46	2.3	2.7			7.81				7.25	11.81	6.08		2.76	5269		
MOL-3	*Limestone moleanos*	wt%	0.678	55	41			0.61	1.54	0.68		0.16	0.02	0.01	0.13	0.0003	0.003	1.98E−05	
		Rel. Unc.%	2.94	2.5	3.3			7.49	5.42	4.71		5.25	6.04	6.93	3.61	2.91	4122	5.02	
LiOZ-1	*Limestone lioz*	wt%	0.183	54	45			0.27		0.27				0.01		3.37E−05			
		Rel. Unc.%	2.48	2.2	2.7			10.11		6.70				5.39		4.28			
LiOZ-2	*Limestone lioz*	wt%	0.567	54	41		0.10		1.38	2.00			0.03		0.19	0.0003		3.80E−05	
		Rel. Unc.%	3.51	3.1	4.2		6.21		4.57	5.08			7.20		7.33	3.52		6.59	
LiOZ-3	*Limestone lioz*	wt%	0.278	54	45		0.03	0.26	0.25	0.57			0.01		0.07	6.45E−05	0.004	4.14E−06	
		Rel. Unc.%	2.47	2.2	2.6		5.52	12.54	6.23	4.89			7.44		7.12	3.18	4476	8.65	
BT	*Limestone tavira*	wt%	0.293	54	43			1.59	0.81				0.01	0.01	0.16	0.0002	0.008	3.49E−05	4.36E−05
		Rel. Unc.%	2.42	2.2	2.7			5.75	3.67				7.02	4.46	3.07	2.35	3146	3.73	5.55
MNR	*Marble ruivina*	wt%	0.084	51	45		0.05	0.47		3.70			0.01	0.01	0.10	6.0E−05	0.003	8.92E−06	

Table 2 (continued)

Sample	Sample type		H2O	CaO	CO2	Na2O	K2O	MgO	Al2O3	SiO2	P2O5	SO3	TiO2	MnO	Fe2O3	B	Cl	Sm	Gd
		Rel. Unc.%	2.80	2.3	2.7		4.33	7.05		3.06			8.34	7.38	8.71	3.26	4565	8.00	
MAL	*Marble alandroal*	wt%	0.126	54	44		0.10	0.60		1.06			0.01	0.01	0.17	5.60E−05	0.002	1.54E−05	
		Rel. Unc.%	2.59	2.2	2.7		3.20	7.13		3.83			7.38	6.23	5.08	3.49	6107	7.16	
MBC	*Marble borba*	wt%	0.185	56	42			0.61	0.75	0.66			0.01	0.02	0.08	3.15E−05	0.002	9.73E−06	
		Rel. Unc.%	2.52	2.0	2.7			6.56	3.06	4.08			7.65	4.48	5.13	4.01	4403	8.34	
MER	*Marble estremoz*	wt%	0.107	54	44			0.45	1.32	0.64			0.01	0.02	0.07	5.12E−05		2.15E−05	2.33E−05
		Rel. Unc.%	3.06	2.4	3.0			9.86	4.75	5.26			10.73	5.60	6.97	2.87		6.46	6.63

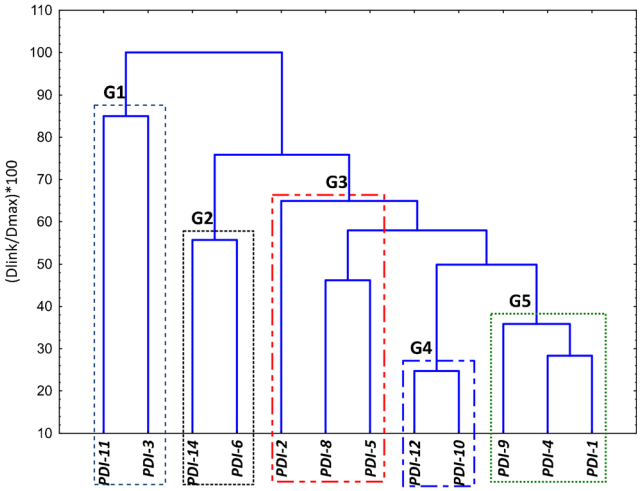

Fig. 7 Tree clustering diagram by using the unweighted pair-group average as amalgamation linkage rule and the Euclidean distances as distance measure (after remove PDV 7 and PDI 13—extreme outliers)

Perdigões site (Dias et al. 2005). More than a half (57%) appear to have been made with marbles from the triangle Estremoz–Borba–Vila Viçosa. Only one artefact, the only stone vessels analysed by PGAA, point to long-distance procurement (in particular MCE limestones). The rest (G1 and G2) do not match with the analysed raw materials and are from unknown sources. Although the number of analysed possible sources represents the carbonate materials' availability, we are aware of the need to increase the number of samples, especially due to local variation. Still, the obtained results allow some important considerations regarding the provenance of these items and their differences between the funerary contexts in Perdigões, obtained with a non-destructive method of analysis to differentiate carbonate rich materials.

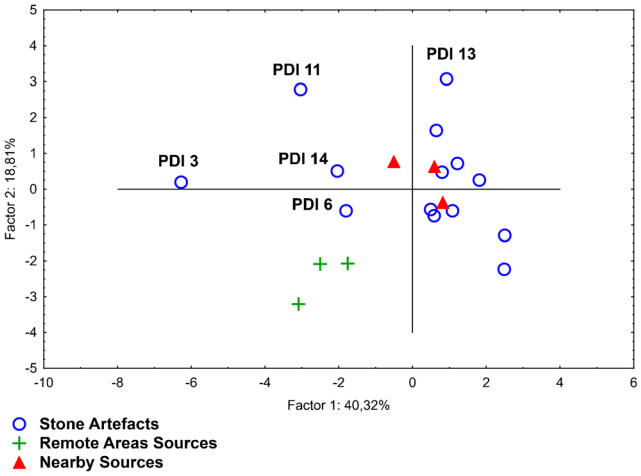

Fig. 8 Projection of the artefacts and potential raw materials on the factor-plane 1 and 2 by using the chemical elements contents obtained by PGAA as variables (after remove Ruivina marble and Tavira breccias—extreme outliers)

Conclusions

Prompt gamma activation analyses proved to be a successful method to distinguish between marble/limestone samples originating from different known geological sources, as well as matching artefacts to sources, when non-destructive analysis is a requisite.

PIXE results were very useful confirming the surface "contamination" of the stone artefacts, particularly the nature of the residues found close to some idols, and in the interior of some vases, particularly with bones, soil residues and ferruginous crusts.

Neutron radiography became more useful in the vase morphological study, with a good observation of the shape and inner structure of each vase but was not very useful in the stone idols analysis, as they are too thick for any differentiation.

This analytical approach supports archaeological inferences using the patterns of chemical composition, contexts, materials types and distribution. No stone idols (between the 13 analysed) from the contexts with cremated remains is related to the Estremadura or Algarve analysed sources. The majority are from the nearby area of Estremoz–Borba–Vila Viçosa, some 30–40 km north of Perdigões, and the rest are from unknown sources. The traditional idea that these objects in Alentejo might have come from the Lisboa Peninsula is now nuanced. On the other hand, the vessel from the tholoi tomb (PDV 7) is compatible with the Estremadura limestones. This seems to suggest that, not just the tholoi tombs and the pits with cremations present different architectures, different body treatments, different material assemblages, but that these particular sets of object have also different raw materials with different provenances (we should note that the other stone vessels and idols from the tholoi tombs are also made of limestone). These results support that imported foreign materials were used in parallel with regional available materials. The object that points to the Lisbon peninsula limestones is of a different typology category—vase—and it was found in the tholoi tomb 1, which presents different funerary procedures from the contexts of provenance of the stone idols.

In this work, different idol types were analysed, diverse types of eyed-cylindrical idols, tolva type idols and small vases, but no specific correlation between typology and raw material was found, with the exception of the analysed vase.

The idols with unknown attribution of raw materials, as well as, the correlated with nearby sources, do not belong to a specific typology. Only the vase point to a long distance source. So, no correlation was established between stylistic differentiations and specific regions.

Different raw material provenances seem to be associated with different contexts and rituals, deepening the contrasts that we can see between these funerary features in Perdigões Chalcolithic archaeological site.

The number of trace elements that can be measured by PGAA is restricted, as well as conclusions, especially when dealing with such heterogeneous geological sources. However, interpretations of the obtained data may be used for general assessments of provenance.

This study enhances the potential of this non-invasive approach to contribute for a better differentiation between carbonate stone-rich artefacts. Though, to establish a better correlation between raw material/artefact types/provenance area, a broader study needs to be performed, including both various stone idol/vase typologies and nearby and long-distance raw material sources. Particular attention should be taken to stone idols found in other southern Iberian Chalcolithic sites, like La Pijotilla, and a comparison between the two sites' artefacts would be interesting, as it was already found interactions in the Chalcolithic between these two sites, particularly for bell-beakers (Odriozola et al. 2008).

This study shows that this line of inquiry has potential to contribute to the definition of the spatiality of an archaeological site, like Perdigões, interaction network and to the characterization of the diversity existing between the several funerary contexts already excavated at a site.

Acknowledgements C2TN/IST authors gratefully acknowledge the FCT support through the UID/Multi/04349/2013 project. Special thanks also to the CHARISMA project cofunded by the European Commission within the action "Research Infrastructures" of the "Capacities", at Budapest Neutron Center, GA No. FP7-228330.

References

Allmäe R, Limbo-Simovart JU, Heapost L, Verš E (2012) The content of chemical elements in archaeological human bones as a source of nutrition research. Pap Anthropol XXI:27–49

Anderson IS, McGreevy RL, Bilheux HZ (2009) Neutron imaging and applications. Springer Verlag, NewYork

Attanasio D, Boschi C, Bracci S, Cantisani E, Paolucci F (2015) Provenance studies of the marble of ancient sculptures in the tribune of the Uffizi gallery, Florence. Archaeometry 57(S1):74–89

Banner JL (1995) Application of the trace element and isotope geochemistry of strontium to studies of carbonate diagenesis. Sedimentology 42:805–824

Beltrán J, Loza Azuaga ML, Ontiveros Ortega E, Rodríguez Gutiérrez O, Taylor R (2012) The quarrying and use of Marmora in Baetica. An Archaeometry-based Research Project. Italica 1:220–229

Cabral JMP, Vieira MCR, Carreira PM, Figueiredo MO, Pena TPA, Tavares A (1992) Preliminary study on the isotopic and chemical characterization of marbles from Alto Alentejo (Portugal). In: Waelkens M, Herz N, Moens L (eds). Ancient stones: quarrying, trade and provenance: interdisciplinary studies on stones and stone technology in Europe and Near East from the Prehistoric to the Early

Christian Period, vol 4. Leuven University Press, Acta Archaeologica Lovaniensia Monographiae, Leuven, pp 191–198
Campbell JL, Hopman TL, Maxwell JA, Nejedly Z (2000) The Guelph PIXE software package III: alternative proton database. Nucl Instr Meth B 170:193–204
Crandell O (2012) Evaluation of PGAA data for provenance of lithic artifacts, Studia UBB. Geologia 57(1):3–11
Dias MI, Prudêncio MI, Valera AC, Lago M, Gouveia MA (2005) Composition, technology and functional features of Chalcolhitic pottery from Perdigões, Reguengos de Monsaraz (Portugal), a preliminary report. Geoarchaeological and Bioarchaeological Studies, Amsterdam, Netherlands 3:161–164
Domínguez Bella S (2009) Huellas de cantería romana de mármol en Almadén de la Plata (Sevilla), un patrimonio a conservar Nogales T, Beltrán J. (coords.), Marmora Hispana: Explotación y uso de los materiales pétreos en la Hispania Romana, Roma, 377–390
Ehinola OA, Ejeh OI, Oderinde OJ (2016) Geochemical Characterization of the Paleocene Ewekoro Limestone Formation, SW Nigeria: Implications for Provenance, Diagenesis and Depositional Environment. Geo-materials 6:61–77. doi:10.4236/gm.2016.63006
Fazekas B, Molnár G, Belgya T, Dabolczi L, Simonits A (1997) Introducing HYPERMET-PC for automatic analysis of complex gamma-ray spectra. J Radioanal Nucl Chem 215:271–277
Goldschmidth JR, Graff L, Joensu OI (1955) The occurrence of magnesium calcite in nature. Geochim Cosmochim Acta 1:212–230
Gyódi I, Demeter I, Hollós-Nagy IK, Kovács I, Szőkefalvi-Nagy Z (1999) External-beam PIXE analysis of small sculptures. Nucl Instr Meth B 150:605–610
Hurtado V. (2008) Ídolos, estilos y territorios de los primeros campesinos en el sur peninsular. In: C. Cacho Quesada, R. Maicas Ramos, J. A. Martos y Mª I. Martínez (coord.). Acercándonos al pasado. Prehistoria en 4 actos. Ministerio de Cultura. Museos Estatales. Museo Arqueológico Nacional y CSIC. Edición en CD y web del MAN. http://man.mcu.es/museo/JornadasSeminarios/acercandonos_al_pasado.html
Hurtado V (2010) "Representaciones simbólicas, sitios, contextos e identidades territoriales en el Suroeste Peninsular", Ojos que nunca se cierran: Ídolos en las primeras sociedades campesinas: 16 de Deciembre de 2009. Museo Arqueológico Nacional, Madrid, pp 137–198
Kasztovszky Z, Biró KT, Markó A, Dobosi V (2008) Archaeometry, cold neutron prompt gamma activation analysis—a non-destructive method for characterization of high silica content chipped stone tools and raw materials. Archaeometry 50(1):12–29
Kis Z, Szentmiklósi L, Belgya T (2015) NIPS–NORMA station—a combined facility for neutron-based non-destructive element analysis and imaging at the Budapest Neutron Centre. Nucl Instr Meth A 779:116–123
Koralay T, Kilinçarslan S (2015) Minero-petrographic and isotopic characterization of two antique marble quarries in the Denizli region (western Anatolia, Turkey). Periodico di Mineralogia 84(2):263–288
Lapuente P (1995) Mineralogical, petrographical and geochemical characterization of white marbles from Hispania, Y. Maniatis, N. Herz and Y. Basiakos (coords.), The Study of Marble and Other Stones Used in Antiquity, London, pp 151–160
Lapuente P, Turi B (1995) Marbles from Portugal: petrographic and isotopic characterization. Sci Technol Cult Herit 4(2):33–42
Mañas Romero I (2012) Marmora de las canteras de Estremoz, Alconera y Sintra: su uso y difusión, Ed. V. García-Entero. El marmor en Hispania: explotación, uso y difusión en época romana, UNED, Madrid, pp 331–346
Martins R, Lopes L (2011) Mármores de Portugal. Rochas & Equipamentos 100:32–56
Morbidelli P, Tucci P, Imperatori C, Polvorinos A, Preite Martinez M, Azzaro E, Hernandez MJ (2007) Roman quarries of the Iberian peninsula: 'Anasol' and 'Anasol'- type. Eur J Mineral 19(1):125–135
Odriozola CP, Hurtado V, Dias MI, Valera AC (2008) Produção e consumo de campaniformes no vale do Guadiana: uma perspectiva ibérica. Eds. NIA-Era Arqueologia. Apontamentos de Arqueologia e Património 3:45–52
Onimisi M, Obaje NG, Daniel A (2013) Geochemical and petrogenetic characteristics of the marble deposit in Itobe area, Kogi state, Central Nigeria. Adv Appl Sci Res 4(5):44–57
Origlia F, Gliozzo E, Meccheri M, Spangenberg JE, Turbanti Memmi I, Papi E (2011) Mineralogical, petrographic and geochemical characterisation of white and coloured Iberian marbles in the context of the provenancing of some artefacts from Thamusida (Kenitra, Morocco). Eur J Mineral 23:857–869
Polvorinos del Río A, Arnedo MJH, Hurtado Pérez V, López JÁ, González MF, Gómez R (2010) Variabilidad espectral VIS-SWIR de objetos líticos de carácter cultual en el yacimiento calcolítico de la Pijotilla. Actas - VIII Congreso Ibérico de Arqueometria. Eds. Carrasco ME, Romero RL, Dias-Tendero MA, Garcia, JC. Teruel, Spain, pp 379–386
Prudêncio MI, Roldán C, Dias MI, Marques R, Eixea A, Villaverde V (2016) A micro-invasive approach using INAA for new insights into Palaeolithic flint archaeological artefacts. J Radioanal Nucl Chem 308:195–203. doi:10.1007/s10967-015-4294-z
Rehren T, Belgya T, Jambon A, Káli G, Kasztovszky Z, Kis Z, Kovács I, Maróti B, Martinón-Torres M, Miniaci G, Pigott VC, Radivojević M, Rosta L, Szentmiklósi L, Szökefalvi-Nagy Z (2013) 5,000 years old Egyptian iron beads made from hammered meteoritic iron. J Archaeol Sci 40:4785–4792
Révay Z (2009) Determining elemental compositions using prompt γ activation analysis. Anal Chem 81:6851–6859
Révay Z, Belgya T (2004) Principles of PGAA method. In: Molnár GL (ed) Handbook of prompt gamma activation, analysis with neutron beams. Kluwer Academic Publishers, Dordrecht, pp 1–30
Révay Z, Firestone RB, Belgya T, Molnár GL (2004) Prompt gamma-ray spectrum catalog. In: Molnár GL (ed) Handb. Prompt gamma act. Anal. Neutron beams. Springer US, Boston, pp 173–364
Révay Z, Belgya T, Molnár GL (2005) Application of Hypermet-PC in PGAA. J Radioanal Nucl Chem 265:261–265
Rosen O, Desmons J, Fettes D (2007) Metacarbonate and related rocks. Provisional recommendations by the IUGS sub-commission on the systematics of metamorphic rocks. Web Version of 1.07. https://www.bgs.ac.uk/scmr/docs/papers/paper_7.pdf.Accessed 02 May 2016
Schindelin J, Arganda-Carreras I, Frise E, Kaynig V, Longair M, Pietzsch T et al (2012) Fiji: an open-source platform for biological-image analysis. Nat Method 9:676
Szentmiklósi L, Belgya T, Révay Z, Kis Z (2010) Upgrade of the prompt gamma activation analysis and the neutron-induced prompt gamma spectroscopy facilities at the Budapest research reactor. J Radioanal Nucl Chem 286:501–505
Taelman D (2014) Contribution to the use of marble in central-Lusitania in roman times: the stone architectural decoration of Ammaia (São Salvador da Aramenha, Portugal). Archivo Español de Arqueologia: 175–194
Taelman D, Elburg M, Smet I, De Paepe P, Luís L, Vanhaecke F, Vermeulen F (2013) Roman marble from Lusitania: petrographical and geochemical characterisation. J Archaeol Sci 5:2227–2236
Taylor ST, McLennan SM (1981) The composition and evolution of the continental crust: rare earth element evidence from sedimentary rocks. Philos Trans R Soc Lond A 301:381–399
Todd TW (1966) Petrographic classification of carbonate rocks. J Sediment Petrol 36(2):317–340
Ulens K, Moens L, Dams R (1994) Study of element distributions in weathered marble crusts using laser ablation inductively coupled plasma mass spectrometry. J Anal At Spectrom 9:1243–1248
Valera AC (2012a) Ditches, pits and hypogea: new data and new problems in South Portugal Late Neolithic and Chalcolithic

funerary practices. In: Gibaja JF, Carvalho AF, Chambom P (eds) Funerary Practices from The Mesolithic to The Chalcolithic of the Northwest Mediterranean, vol 2417. BAR International Series, Oxford, pp 103–122

Valera AC (2012b) Mind the gap: Neolithic and Chalcolithic enclosures of South Portugal. In: Gibson A (ed) Enclosing the Neolithic. Recent studies in Britain and Europe, vol 2440. BAR International Series, Oxford, pp 165–183

Valera AC (2015) The diversity of ideotechnic objects at Perdigões enclosure: a first inventory of items and problems. Arpi 3:238–256

Valera AC, Silva AM, Márquez Romero JEM (2014a) The temporality of Perdigões enclosures: absolute chronology of the structures and social practices. SPAL 23:11–26

Valera AC, Silva AM, Cunha C, Evangelista LS (2014b) Funerary practices and body manipulations at Neolithic and chalcolithic Perdigões ditched enclosures (South Portugal). In: Valera AC (ed) Recent prehistoric enclosures and funerary practices, vol 2676. BAR International Series, Oxford, pp 37–57

Wavemetric Inc., IGORPro (2013) 10200 SW Nimbus, G-7 Portland, OR97223 USA, http://www.wavemetrics.com/products/igorpro/